PHYSICAL REVIEW B VOLUME 22, NUMBER 8 15 OCTOBER 1980

Time development of the spectral redistribution in disordered systems with a Lorentzian transfer rate: Theoretical models and a Monte Carlo study

S. K. Lyo
Sandia Laboratories, Albuquerque, New Mexico 87185*
(Received 25 March 1980)

The time-dependent spectral redistribution in fluorescence line narrowing in an inhomogeneously broadened system is investigated by means of simple theoretical models and Monte Carlo calculations. The two-site phonon-assisted energy transfer rate is assumed to be site-symmetric and a Lorentzian function of energy mismatch. For the Monte Carlo calculations initial excitations are made at the wing, shoulder, and center of the inhomogeneously broadened Gaussian band. For the wing excitation it is argued that, because of the above Lorentzian factor, the intensity in the initial site of excitation decays with a much smaller back-transfer rate than for the center excitation, simplifying the theoretical treatment. This effect is demonstrated by the Monte Carlo study. A refinement of this model is developed for a general situation, and its predictions are compared with the Monte Carlo results.

I. INTRODUCTION

With the recent development of a fluorescence-line-narrowing technique there has been growing interest[1-5] in the phenomena of time-dependent spectral transport in inhomogeneously broadened systems. Time-resolved studies of the fluorescence of an initially narrow spectral line after a laser excitation provide important information about the spectral and spatial dynamics of optical excitations in a disordered system with a random distribution of the positions and energy levels of the optically active ions.

In previous studies[1-4] the spectral and spatial transport has been investigated for simple systems such as $LaF_3:Pr^{3+}$ where the elemental two-site phonon-assisted energy transfer rate is independent of energy mismatch. In the present work we study another class of systems where the transfer rate has a Lorentzian dependence on energy mismatch. The rate is site-symmetric when the thermal energy is much larger than the inhomogeneous broadening. For example, such a rate is obtained for two-phonon–assisted processes[6] where phonon emission and absorption occur at the same site. According to the spectral overlap method,[7] the transfer rate is proportional to the convolution of the emission profile of one site with the absorption profile of the other. Therefore for Lorentzian line-shape functions the rate is a Lorentzian function of energy mismatch with a width equal to twice the homogeneous width.

Theoretical models for the time evolution of the spectral profile are developed by ignoring the radiative decay. The latter can be accounted for in a trivial way. The "exact" solutions are then obtained by performing a full Monte Carlo calculation. The latter takes into account the microscopic spatial (i.e., topological) correlations of the impurity sites. The accuracy of the theoretical models is assessed by comparing the theoretical predictions with the Monte Carlo results.

II. GENERAL FORMALISM OF SPECTRAL TRANSPORT

In this section we set up a general formalism for the time-dependent spectral transfer in a system where the transfer rate has an arbitrary dependence on energy mismatch. The intensity of fluorescence at energy E and time t is proportional to the spectral function

$$P(E,t) \equiv \sum_i n_i(t)\delta(E-E_i)\,, \tag{2.1}$$

where $n_i(t)$ and $\delta(x)$ are the probability that an ith ion with an energy level E_i is excited and Dirac's delta, respectively. The initial spectral profile $P(E,0)$ is sharply peaked at a certain energy.

By separating the contributions from sites initially excited in (2.1), one can transform (2.1) into a more illuminating expression for an infinitely large system (see the Appendix):

$$\begin{aligned} P(E,t) = {} & \chi(E,t)P(E,0) \\ & + \{I_0[1-\chi(E,t)]/N - \langle n'(E,t)\rangle\} P(E,0) \\ & + \langle n'(E,t)\rangle g(E)\,, \end{aligned} \tag{2.2}$$

where

$$\chi(E,t) = \langle n^0(E,t) - I_0/N\rangle/(1-I_0/N)\,. \tag{2.3}$$

Here, $g(E)$, $I_0 \equiv \int P(E,0)dE$, and $N \equiv \int g(E)dE$ are the distribution function of the impurity levels, total number of ions initially excited, and total number of ions in the sample, respectively. The quantity $\langle n^0(E,t)\rangle$ $[\langle n'(E,t)\rangle]$ represents the spatially averaged probability that a site with an energy level E initially excited (not excited) will be in an excited state at time t. The function $\chi(E,t)$ then describes the average decay of the

initially excited ions of energy E into the equilibrium situation, $P(E,\infty)$. The function $\chi(E,t)$ decays monotonically from $\chi(E,0)=1$ to $\chi(E,\infty)=0$, and $\langle n'(E,t)\rangle$ grows from $\langle n'(E,0)\rangle=0$ to $\langle n'(E,\infty)\rangle=I_0/N$. Note that the expression in (2.2) reduces to $P(E,0)$ at $t=0$ and to the equilibrium state $P(E,\infty)=I_0 g(E)/N$ at $t=\infty$ as is expected. If the transfer rate is independent of energy mismatch, the quantities $\chi(E,t)$ and $\langle n'(E,t)\rangle$ become independent of energy. Using conservation of intensity, one finds $\langle n'\rangle = I_0(1-\chi)/N$ in (2.2), and the second term on the right-hand side vanishes. This result was obtained earlier.[3]

When only a small fraction of ions are excited (i.e., $I_0/N \ll 1$), the second term on the right-hand side in (2.2) can be neglected, yielding

$$P(E,t)=\chi(E,t)P(E,0)+\langle n'(E,t)\rangle g(E)\,. \tag{2.4}$$

The term proportional to $P(E,0)$ in (2.4) represents the decay of the initial line and the last term the recovery of the equilibrium background.

The time-dependent spectral profile is determined by the quantities $\chi(E,t)$ and $\langle n'(E,t)\rangle$. These quantities are calculated from the master equation[8] ($W_{ii}\equiv 0$)

$$dn_i(t)/dt=\sum_j W_{ij}\,[n_j(t)-n_i(t)]\,, \tag{2.5}$$

where the transfer rate is given by

$$W_{ij}=W_{ji}=R(r_{ij})f(E_{ij})\,. \tag{2.6a}$$

For a single-site excitation the initial conditions read $n_i(0)=\delta_{i,0}$. Here δ is Kronecker's delta and 0 denotes the initial site. A Lorentzian dependence on energy mismatch E_{ij} will be assumed for $f(E_{ij})$:

$$f(E_{ij})=\frac{\gamma^2}{(E_i-E_j)^2+\gamma^2}\,. \tag{2.6b}$$

Here γ is a constant. In (2.6a) the function $R(r_{ij})$ depends only on the spatial separation r_{ij} between sites i and j. For an electrostatic multipole interaction, R is given by

$$R(r_{ij})=b\left(\frac{a}{r_{ij}}\right)^{\alpha}, \tag{2.6c}$$

where b is a rate constant and the length a is defined by $c=\rho a^3$. Here c and ρ are the concentration and density of the optical ions. For a simple cubic lattice a becomes the lattice constant. In (2.6c) $\alpha=6$, 8, and 10, respectively, for dipole-dipole, dipole-quadrupole, and quadrupole-quadrupole interactions.

III. THEORETICAL MODELS

In this section we present theoretical models for $\chi(E,t)$ and $\langle n'(E,t)\rangle$. The approach adopted here is a generalization of the idea developed in previous works[4] for simple systems where the transfer rate is independent of energy mismatch. For simplicity we assume a single-site excitation.

A. Decay without back transfer: wing excitation

For a simple lowest-order approximation for $\chi(E,t)$, we regard the initial site (to be designated as the 0th site) as a donor and the rest of the ions as acceptors and ignore back transfer from the acceptors to the donor.[9] This picture is expected to be especially relevant for the case of the wing excitation. In this situation the excitation in the initial site prefers to jump to a (spatially) neighboring ion, because the rate decays more rapidly with range than with energy separation. The neighbor ion, however, is likely to have an energy level near the center of the band because of the large density of states there. Once the excitation makes a transition from the initial site at the wing to the neighboring ion near the center of the band, the probability that it will come back to the initial site is much smaller for the case of a wing excitation than for a center excitation for the following reason. The new excited ion (with energy near the center of the band) is likely to be surrounded by ions with energy levels near the center of the band (the initial ion is not necessarily the nearest neighbor to the new site) and the back-transfer rate from the new site (now assumed to be near the center of the band) to the wing is reduced according to the Lorentzian weighting factor in (2.6b) compared with the transfer rate to its other neighbors which are likely to be near the center of the band. However, for an initial center excitation, the Lorentzian factor does not have such a discriminatory effect against back transfer to the initial site. Note that this effect does not obtain when the transfer rate is independent of energy mismatch.

Dropping I_0/N in (2.3) and ignoring the first term on the right-hand side of (2.5), one finds

$$\chi(E,t)=\left\langle \exp\left(-\sum_{i=1}^{N-1} W_{0i}\,t\right)\right\rangle = \prod_{i=1}^{N_0-1}\{1-c[1-\langle \exp(-W_{0i}t)\rangle_{E_i}\}\,, \tag{3.1a}$$

where $E=E_0$, $\langle\,\rangle_{E_i}$ denotes an averaging on the energy distribution of E_i, and N_0 is the total number of lattice sites in the sample. At a low concentration (i.e., $c\ll 1$), (3.1a) reduces to

$$\chi(E,t)=\exp\left(-c\sum_{i=1}^{N_0-1}\,[1-\langle\exp(-W_{0i}t)\rangle_{E_i}]\right). \tag{3.1b}$$

Employing a continuum approximation and using

(2.6a) and (2.6c), one finds

$$\chi(E,t)=\exp\left[-\frac{4\pi c}{3}f_\alpha(E)\Gamma\left(1-\frac{3}{\alpha}\right)(bt)^{3/\alpha}\right], \quad (3.2)$$

where $\Gamma(x)$ is a gamma function and

$$f_\alpha(E)=\langle[f(E-E_i)]^{3/\alpha}\rangle_{E_i}. \quad (3.3)$$

Evaluation of $\langle n'(E)\rangle$ is not easy even for this simple model. As will be discussed later, the quantity $\chi(E,t)$ can readily be extracted out from the data for the wing excitation and this provides a sufficient amount of information.

B. Direct transfer model

The model discussed above is not adequate for the case of a laser excitation near the center of the band. The effect of back transfer to the initial site of excitation has to be considered. In the following, we study a simple soluble model which accommodates such an effect at least for a short time. In this model, we allow energy transfer (including back transfer) between the donor (i.e., the initial site) and the acceptors (i.e., other ions), and ignore the secondary transitions among the latter in the time interval during which this approximation is valid.

The transport equation of this model is given by

$$\frac{dn_0}{dt}=\sum_i W_{0i}n_i-\sum_i W_{i0}n_0, \quad (3.4a)$$

$$\frac{dn_i}{dt}=W_{i0}n_0-W_{0i}n_i. \quad (3.4b)$$

Introducing the Laplace transform $n_i(s)=\int e^{-st}n_i(t)dt$, one has

$$n_i(s)=W_{0i}n_0(s)/(s+W_{0i}) \quad (i\neq 0) \quad (3.5a)$$

$$n_0(s)=\left(s+\sum_{i'}\frac{sW_{0i'}}{s+W_{0i'}}\right)^{-1}. \quad (3.5b)$$

The expression in (3.5a) can be rewritten with (3.5b) as $(i\neq 0)$

$$n_i(s)=\int_0^\infty dx\, e^{-xs}\frac{W_{0i}}{s+W_{0i}}\times\exp\left(-\frac{xsW_{0i}}{s+W_{0i}}\right)\prod_{i'\neq i}^{N}\exp\left(-\frac{xsW_{0i'}}{s+W_{0i'}}\right). \quad (3.6)$$

Employing low concentration and continuum approximations and setting $E=E_i$, one finds

$$\langle n'(E,s)\rangle\equiv\langle n_i(s)\rangle=\frac{4\pi c}{3N}\int_0^\infty dx\, e^{-xs}\int_0^\infty dp\, Q_\alpha(p,E)\exp[-xsQ_\alpha(p,E)]\times\exp\left(-\frac{4\pi c}{3}\left\langle\int dp'\{1-\exp[-xsQ_\alpha(p',E_{i'})]\}\right\rangle_{E_{i'}}\right), \quad (3.7)$$

where

$$Q_\alpha(p,E)=[1+sb^{-1}p^{\alpha/3}/f(E_0-E)]^{-1}. \quad (3.8)$$

The expression in (3.7) is simplified on integrating by parts in x, yielding

$$\langle n'(E,s)\rangle=\frac{[f(E_0-E)]^{3/\alpha}}{Nf_\alpha(E_0)}\left(\frac{1}{s}-\chi(E_0,s)\right), \quad (3.9)$$

with

$$\chi(E_0,s)=\frac{1}{s}\int_0^\infty dx\, e^{-x}\exp[-(sb^{-1})^{3/\alpha}f_\alpha(E_0)G_\alpha(x)] \quad (3.10)$$

and

$$G_\alpha(x)=\frac{8\pi x}{3}\int_0^{\pi/2}\cos\theta\sin\theta(\tan\theta)^{6/\alpha}\times\exp(-x\cos^2\theta)\,d\theta. \quad (3.11)$$

Performing the inverse Laplace transform for (3.9) and integrating over the initial spectral function

$$\langle n'(E,t)\rangle=\frac{1}{N}\int P(E_0,0)[f(E_0-E)]^{3/\alpha}\times[1-\chi(E_0,t)]/f_\alpha(E_0)\,dE_0. \quad (3.12a)$$

For $\alpha=6$, the function $\chi(E,t)$ is given by[4]

$$\chi(E,t)=\frac{2}{\pi}\int_0^\infty dx\, e^{-x}\int_0^\infty\frac{\sin z}{z}\exp\left(-\frac{[cf_6(E)G_6(x)\sqrt{bt}\,]^2}{z^2}\right)dz. \quad (3.13)$$

For a sharp initial profile $P(E_0, 0) = I_0\delta(E_0 - E_{\text{ini}})$, (3.12a) reduces to

$$\langle n'(E,t)\rangle = \frac{I_0}{N}[f(E_{\text{ini}} - E)]^{3/\alpha}[1 - \chi(E_{\text{ini}}, t)]/f_\alpha(E_{\text{ini}}). \tag{3.12b}$$

C. Pair-decay model

It is expected that the direct transfer model developed in Sec. III B leads to a very slow long-time decay for $\chi(t)$ because the excitation is forced to return to the initial ion after a jump to a new site. Applying the same kind of argument employed earlier to justify the decay without back transfer at the wings, we can neglect back transfer from ions far from the initial site spatially and energetically. For simplicity we allow back transfer only from the first-neighbor ion (to be designated by the subscript 1). The excitation is allowed to diffuse further into the background ions from the first neighbor but without back transfer.

The transport equation is given by

$$\begin{aligned}
\frac{dn_0}{dt} &= -W_0 n_0 + W_{01} n_1, \\
\frac{dn_1}{dt} &= -W_1 n_1 + W_{01} n_0, \\
\frac{dn_i}{dt} &= W_{i0} n_0 + W_{i1} n_1 \quad (i \neq 0, 1),
\end{aligned} \tag{3.14}$$

where $W_i = \sum_k W_{ik}$ $(i = 0, 1)$ is the total transition rate from site i and $n_i(0) = \delta_{i,0}$. The solutions for (3.14) read

$$\begin{aligned}
n_0(t) &= \tfrac{1}{2}\sum_{\pm}\left(1 \pm \frac{W_0 - W_1}{2D}\right)\exp\left[-\left(\frac{W_0 + W_1}{2} \pm D\right)t\right], \\
n_1(t) &= \frac{W_{01}}{2D}\sum_{\pm} \mp \exp\left[-\left(\frac{W_0 + W_1}{2} \pm D\right)t\right], \\
n_i(t) &= \tfrac{1}{2}\sum_{\pm}\left(\frac{W_0 + W_1}{2} \pm D\right)^{-1} \\
&\quad \times \left\{1 - \exp\left[-\left(\frac{W_0 + W_1}{2} \pm D\right)t\right]\right\} \\
&\quad \times \left(1 \pm \frac{W_0 - W_1}{2D} \mp \frac{W_{01}}{D}\right) \quad (i \neq 0, 1),
\end{aligned} \tag{3.15}$$

where $D = [W_{01}^2 + \frac{1}{4}(W_0 - W_1)^2]^{1/2}$.

It is difficult to perform the statistical averaging for (3.15) analytically in obtaining the time-dependent spectral function. Therefore a Monte Carlo method will be employed for this purpose. We have chosen 220 random sites in a simple cubic lattice so as to model a 1% concentration. Each impurity site is represented by three random coordinates. To minimize the size effect, the site to be excited initially is chosen at the center of the cube with a desired initial energy level. We then randomly choose a distribution of energy levels from the function $g(E)$ and evaluate (3.15). The procedure is repeated and the ensemble average is carried out for the spectral function. For a transfer rate decaying rapidly with range this method is expected to yield a reasonably accurate result with even a smaller sample size. Note that this method is very simple compared to the full Monte Carlo calculation to be discussed in the next section and costs less computing time than evaluating certain analytic expressions such as (3.13).

IV. MONTE CARLO CALCULATIONS AND DISCUSSIONS

In this section we present the "exact" solutions for the spectral function obtained by a direct numerical evaluation of (2.5) and compare them with the predictions of the theoretical models developed in Sec. III. The system has been prepared according to the description given at the end of Sec. III C for a 1% sample with 220 impurity sites. The distribution function $g(E)$ for the inhomogeneous broadening of the levels is given by the histogram exhibited in Fig. 1. The latter is an approximation for the Gaussian function shown therein by squares. The inhomogeneous band is divided into 49 bins and the energy levels are given integer values $1 \leq E \leq 49$. The width γ in (2.6b) is assumed to be unity. The master equation (2.5) is solved according to the prescription detailed in Ref. 4. A periodic boundary condition is employed to reduce the size

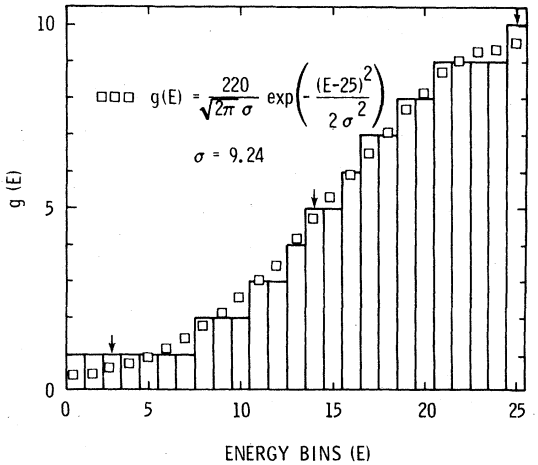

FIG. 1. Histogram representation for the Gaussian function $g(E)$. The inhomogeneous band is divided into 49 bins ($E = 1, 2, \ldots, 49$). Only the left half of the symmetric distribution function including the central bin ($E = 25$) is shown. The arrows indicate the three positions of the initial laser line.

effect. Namely, if the x component (for example) of the vector connecting two impurity sites is larger than half the cube dimension (L), then L is subtracted from the former. An ensemble average is carried out over 400 computer runs. The laser excitation is made at the center ($E=25$), shoulder ($E=14$), and wing ($E=3$), respectively.

The time development of the spectral functions obtained by the full Monte Carlo calculation is shown in Fig. 2. Note that the time scale for the wing excitation is 10 times larger than that for the shoulder and center excitations. The progress of the spectral profile is faster closer to the center of the band, reflecting the Lorentzian dependence of the transfer rate on the energy mismatch and the Gaussian form of the density of states. As has been pointed out following (2.4), the time-dependent spectral profile consists of a contribution representing the decay of the initial line and that representing the recovery of the background. According to (2.4), the latter is proportional to the product of the density of states at energy E and the transition probability from the initial line to E. This effect is clearly seen in Fig. 2. For the center excitation the original sharp line spreads out gradually. However, for the wing excitation the gradual spreading of the initial line does not occur because of the lack of density of states at the tails. Instead, the background begins to emerge pronouncedly near the center where the density of states is large, as is seen for $t=5000$ in Fig. 2. Owing to the Lorentzian form of the rate, the peak appears somewhat to the left of the center. For the shoulder excitation the spectral profile shows a gradual spreading of the line toward the center and at the same time a separate hump near the latter. A similar behavior was seen in the work of Holstein, Lyo, and Orbach[10] based on the Motegi–Shionoya equation,[11,12] and by Huber and Ching (HC).[5] This behavior is in contrast to the situation where the transfer rate is independent of energy mismatch. In this case the full background emerges undistorted while the initial line decays concomitantly.[3]

Experimentally the separation of the spectral profile into the residual initial intensity and that

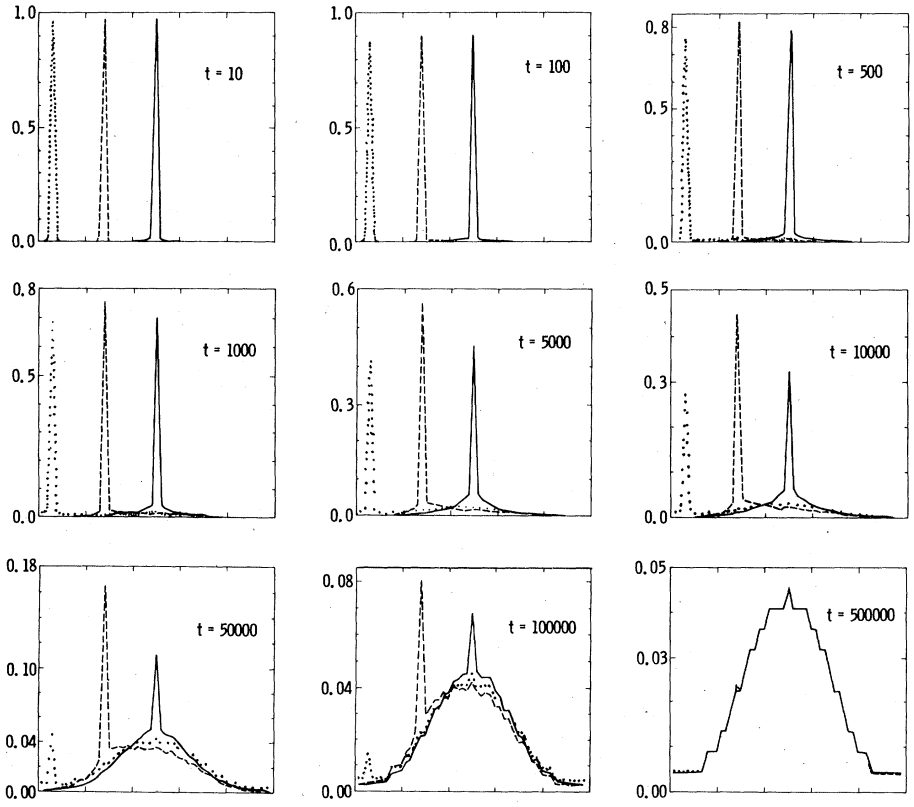

FIG. 2. Time development of the spectral emission line-shape functions. The time is given in units of b^{-1} for center (——) and shoulder (---) excitations and $10b^{-1}$ for the wing (. . .) excitation. The quantity b^{-1} corresponds to the transfer time between two impurities separated by a lattice constant. The area under each curve is conserved and equals unity. The line shape for $t=500\,000$ corresponds nearly to the normalized density of states in Fig. 1. Note the change of vertical scales for successive figures.

arising from the redistribution of the initial line is not easy. However, for a sharp initial line the former can be separated out by subtracting the smooth background from the spectral function. This procedure is particularly simple at the wings where the latter is negligibly small. The theoretical models for $\chi(E,t)$ are compared with the "exact" solution for the wing excitation in Fig. 3. The simple model which ignores back transfer to the initial site gives an impressive agreement with the exact solution, as has been predicted earlier in Sec. III A. The intensity drops to about half within a time $bt=10^4$. This corresponds to the transfer time between two sites with equal energies separated by an average distance at 1% concentration. The situation is less satisfactory for the shoulder excitation (see Fig. 4). Note a nearly complete agreement between the result of the pair model and the exact solution in Fig. 3. The theoretical models are less successful for the center excitation as is evidenced in Fig. 5. However, the pair model can provide a basis for the interpretation of the early-time data. We emphasize here that $\chi(E,t)$ develops faster with time for E closer to the center of the band. This is a strong indication of a transfer rate that falls with increasing energy mismatch. For a transfer rate independent of the latter, $\chi(t)$ will be independent of energy. The theoretical predictions of the spectral function

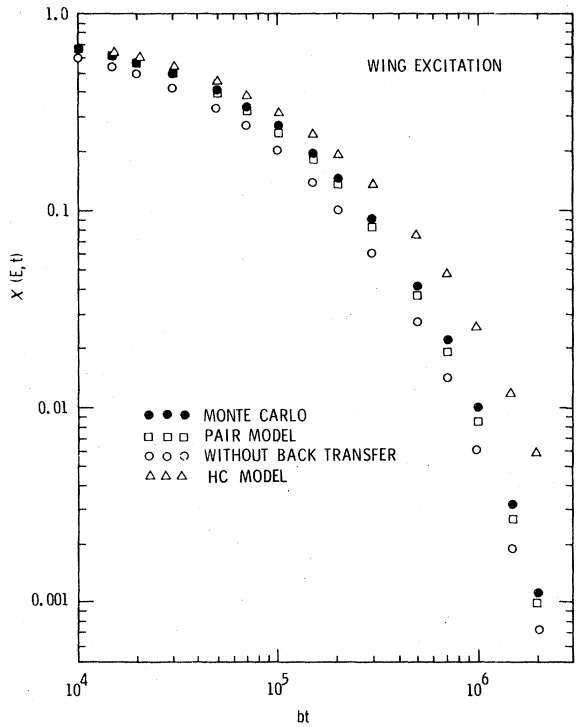

FIG. 3. The theoretical results for $\chi(E,t)$ are compared with the Monte Carlo calculation for the wing excitation ($E=3$).

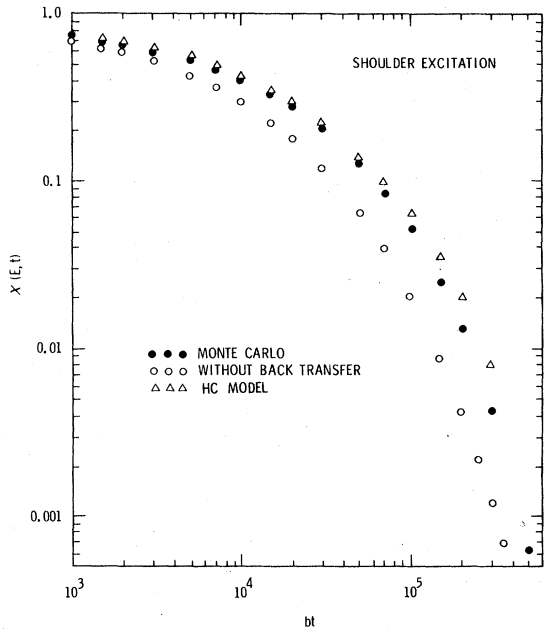

FIG. 4. The theoretical result for $\chi(E,t)$ is compared with the Monte Carlo calculation for the shoulder excitation ($E=14$).

are compared with the Monte Carlo results in Figs. 6–8.

Finally, we compare the present result with the prediction of the HC model.[5] They assume that the effect of back transfer is accounted for approxi-

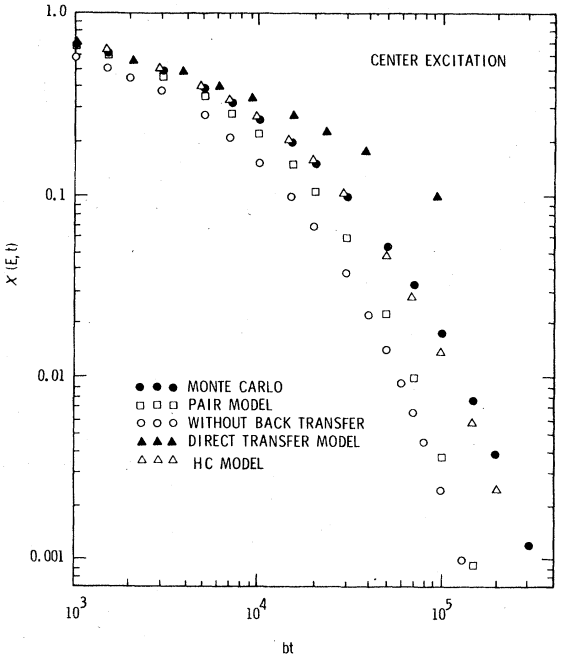

FIG. 5. The results of various theoretical models for $\chi(E,t)$ are compared with the Monte Carlo calculation for the center excitation ($E=25$).

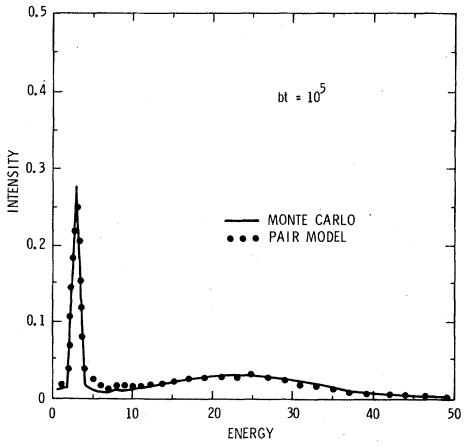

FIG. 6. Comparison of the theoretical result for the spectral function with the Monte Carlo result for the wing excitation.

mately by replacing[5]

$$\exp(-W_{0i}t) \rightarrow \exp(-W_{0i}t)\cosh(W_{0i}t) \qquad (4.1)$$

in (3.1a). When the transfer rate is independent of energy mismatch, it was shown that the assumption in (4.1) is equivalent to the pair-decay model.[4] Noting that (4.1) corresponds to replacing[13] $c \rightarrow \frac{1}{2}c$ and $t \rightarrow 2t$ in (3.1a), one finds from (3.2)

$$\chi_{HC}(E,t) = \chi^{(2^{3/\alpha}/2)}, \qquad (4.2)$$

where χ is given in (3.2).

The predictions of (4.2) are displayed in Figs. 3–5. For the wing excitation, $\chi_{HC}(E,t)$ gives a poor agreement with the exact result. Its prediction is even poorer than the no-back-transfer model. However, it improves significantly with E closer to the center and gives an impressive fit for the center excitation. It is expected that

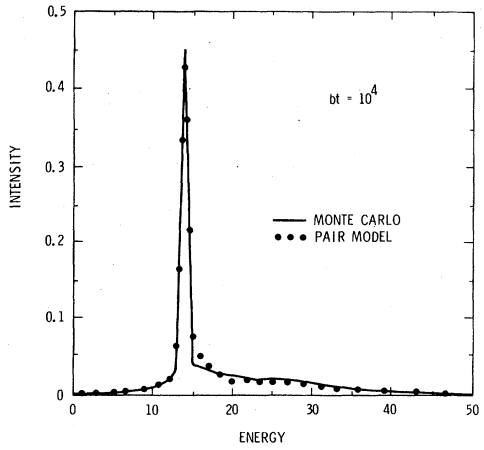

FIG. 7. Comparison of the theoretical result for the spectral function with the Monte Carlo result for the shoulder excitation.

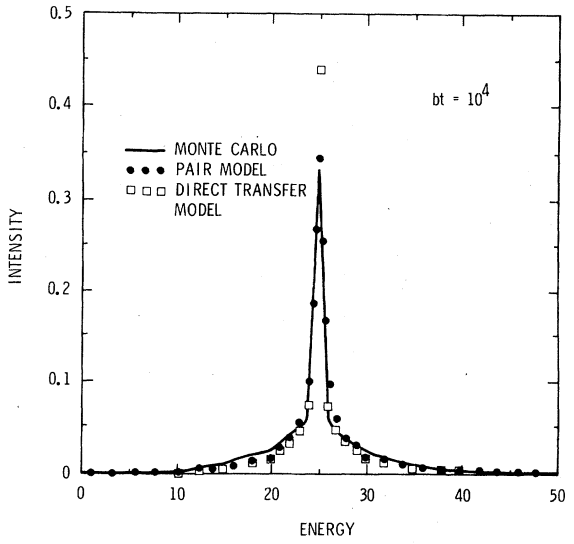

FIG. 8. Comparison of the theoretical result for the spectral function with the Monte Carlo result for the center excitation.

the HC model will yield a similar degree of fitting for the spectral functions shown in Figs. 6–8. Namely, it will give poorer and better agreement, respectively, for the wing and center excitations than for the pair-decay model.

V. CONCLUSION

The time-dependent spectral redistribution in fluorescence line narrowing is studied in an inhomogeneously broadened system. The two-site transfer rate is assumed to be site-symmetric and a Lorentzian function of energy mismatch. The spectral intensity is separated into the residual initial line intensity and the background intensity arising from energy transfer. For the wing excitation it is argued that the intensity in the initial site decays to a lowest-order approximation nearly without back transfer. For a center excitation as well as for the case when the rate is independent of energy mismatch, back transfer is much more important. This effect is demonstrated by the Monte Carlo solution. An improvement of the theoretical model is made by allowing back transfer from the first neighbor of the initial site. Also, an exactly soluble model is examined. We have performed Monte Carlo calculations for initial excitations at the center and shoulder as well as the wing of the inhomogeneously broadened Gaussian band and compared the results with those of the theoretical models.

ACKNOWLEDGMENTS

This work was supported by the U. S. Department of Energy (DOE) under Contract No. DE-AC04-76-

DP00789. The author wishes to thank Professor D. L. Huber and Dr. D. Emin for valuable comments on the manuscript.

APPENDIX

In this appendix we give a brief derivation of (2.2). It is convenient to rewrite (2.1) as

$$P(E,t)=P_1(E,t)+P_2(E,t)\,, \tag{A1}$$

where

$$P_1(E,t)=\sum_{i_0} n_{i_0}(t)\delta(E-E_{i_0})\,, \tag{A2a}$$

$$P_2(E,t)=\sum_{i}{}' n_i(t)\delta(E-E_i)\,. \tag{A2b}$$

In (A2a) the subscript i_0 indicates those sites excited initially [i.e., $n_{i_0}(0)=1$]. The prime in (A2b) means summing over only those sites that are not excited initially. The expression for $P_1(E,t)$ is then recast into an identity

$$\begin{aligned}P_1(E,t)=&\frac{1}{1-I_0/N_0}\sum_{i_0}\left(n_{i_0}(t)-\frac{I_0}{N_0}\right)\delta(E-E_{i_0})\\&+\frac{I_0/N_0}{1-I_0/N_0}\left(\sum_{i_0}\delta(E-E_{i_0})\right.\\&\left.-\sum_{i_0} n_{i_0}(t)\delta(E-E_{i_0})\right).\end{aligned} \tag{A3}$$

The quantity $n_{i_0}(t)$ depends on the energy level E_{i_0}. This explicit dependence will be denoted by $n_{i_0}(t) \equiv n_{i_0}(E_{i_0},t)$. The first term in (A3) can then be rewritten as

$$\frac{1}{1-I_0/N_0}\sum_{i_0}\left(n_{i_0}(E,t)-\frac{I_0}{N_0}\right)\delta(E-E_{i_0})\,. \tag{A4}$$

The sum on i_0 in (A4) is over an infinitely large number of sites resonant at E. Therefore the the quantity in the large parentheses in (A4) can be replaced by its spatial average $\langle n^0(E,t)-I_0/N_0\rangle$. Observing that

$$P(E,0)=\sum_{i_0}\delta(E-E_{i_0})\,, \tag{A5}$$

one identifies (A4) with the first term in (2.2). Similarly, the second term of (A3) yields

$$\frac{I_0/N_0}{1-I_0/N_0}\left[1-\langle n^0(E,t)\rangle\right]P(E,0)\,. \tag{A6}$$

Also, the quantity $P_2(E,t)$ in (A2b) reduces to

$$\begin{aligned}P_2(E,t)&=\langle n'(E,t)\rangle\sum_{i}{}'\delta(E-E_i)\\&=\langle n'(E,t)\rangle[g(E)-P(E,0)]\,.\end{aligned} \tag{A7}$$

The last two terms in (2.2) then follow from (A6) and (A7).

---

*A U. S. Department of Energy facility.

[1]P. M. Selzer, D. S. Hamilton, R. Flach, and W. M. Yen, J. Lumin. 12/13, 737 (1976); P. M. Selzer, D. S. Hamilton, and W. M. Yen, Phys. Rev. Lett. 38, 858 (1977).

[2]D. L. Huber, D. S. Hamilton, and B. Barnett, Phys. Rev. B 16, 4642 (1977); W. Y. Ching, D. L. Huber, and B. Barnett, *ibid.* 17, 5025 (1978).

[3]S. K. Lyo, T. Holstein, and R. Orbach, Phys. Rev. B 18, 1637 (1978).

[4]S. K. Lyo, Phys. Rev. B 20, 1297 (1979); J. Phys. C 12, L83 (1979).

[5]D. L. Huber and W. Y. Ching, Phys. Rev. B 18, 5320 (1978).

[6]T. Holstein, S. K. Lyo, and R. Orbach, Phys. Rev. Lett. 36, 891 (1976).

[7]T. Forster, Ann. Phys. (Paris) 2, 55 (1948); D. L. Dexter, J. Chem. Phys. 21, 836 (1953).

[8]S. Alexander and T. Holstein, Phys. Rev. B 18, 301 (1978).

[9]M. Inokuti and F. Hirayama, J. Chem. Phys. 43, 1978 (1965).

[10]T. Holstein, S. K. Lyo, and R. Orbach, Phys. Rev. B 15, 4693 (1977).

[11]N. Motegi and S. Shionoya, J. Lumin. 8, 1 (1973).

[12]The macroscopic spectral transport equation used in Refs. 10 and 11 requires the quantity $R(r_{ij})$ in (2.6a) to be independent of r_{ij} and can serve only as a crude zeroth-order approach.

[13]A. Blumen, J. Chem. Phys. 72 (4), 2632 (1980).